Optical Power Limiter Using a Saturated SOA-Based Interferometric Switch

N. Pleros, G. T. Kanellos, C. Bintjas, A. Hatziefremidis, and H. Avramopoulos

***Abstract*—We demonstrate an optical power limiter using a semiconductor optical amplifier (SOA)-based interferometric gate powered by a strong continuous-wave input signal. We present a detailed theoretical and experimental investigation of the power limiting characteristics of saturated SOA-based switches, showing good agreement between theory and experiment.**

***Index Terms*—Limiter, optical signal processing, semiconductor optical amplifier (SOA), ultrafast nonlinear interferometer (UNI).**

I. Introduction

OPTICAL signal processing and switching have experienced a remarkable advance during the last years, one main reason for this being the significant progress made on high-speed semiconductor optical amplifier (SOA)-based interferometric gates. However, as the emphasis was rather on enhancing the speed characteristics of optical gates [1], it is still questionable if their functional potential has been fully explored. If electronic circuitry is a guide, power limiting devices, for example, are close relatives to active switching elements as their operation relies on the saturation of the transistors, and their optical high-speed analogue versions would certainly extend the optical signal processing application vistas [2] and improve their performance [3]. So far, SOA-based switches with enhanced input power dynamic range have been presented [4], [5], whereas more recently, we have proposed the use of saturated SOA-based optical gates to demonstrate novel functional subsystems for optical packet switching applications [6], [7]. However, no detailed analysis of the gate's operational potential as an optical power limiter has been presented so far.

In this letter, we demonstrate, for the first time to our knowledge, theoretical and experimental analysis of the power-limiting properties of an SOA-based optical gate saturated by a strong continuous-wave (CW) signal. By using a Mach–Zehnder interferometer (MZI), a novel frequency domain theoretical transfer function approach is derived, indicating that saturated optical switches can provide input pulse power fluctuation suppression in excess of 10 dB. The increased power equalization properties of the gate are explained by the theoretical investigation of its output versus input power transfer function, revealing that output power clips to a constant level for input power levels greater than a specific threshold, when the SOA gain is appropriately biased. Finally, we demonstrate experimental evidence of the power-limiting power transfer function for 10-GHz pulse sequences using the ultrafast nonlinear interferometer (UNI), showing good agreement with the corresponding theoretically obtained curve.

Manuscript received March 23, 2004; revised May 27, 2004.

The authors are with the School of Electrical and Computer Engineering, National Technical University of Athens, Zographou GR15773, Athens, Greece (e-mail: npleros@cc.ece.ntua.gr; gkanel@mail.ntua.gr; cbint@cc.ece.ntua.gr; ahatzi@cc.ece.ntua.gr; hav@cc.ece.ntua.gr).

Digital Object Identifier 10.1109/LPT.2004.833960

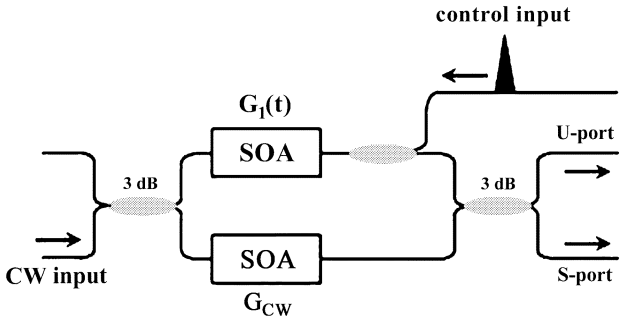

Fig. 1. MZI configuration.

II. Concept and Experiment

The operation of SOA-based interferometric switches as power limiting devices relies on properly biasing the SOA close to its material transparency by a CW input signal, in a way that a π phase shift can be still obtained when a control pulse with appropriate energy level is injected. As such, the output power will increase with the control pulse energy until a π phase shift is obtained, but then greater control pulse energies will cause again an almost π phase shift leading to constant output power, since the SOA operates now at transparency and its gain has reached its unitary end-point.

Fig. 1 shows a typical SOA-based MZI switch [8] arranged in a counterpropagating configuration. A CW signal and a pulsed optical beam are used as the input and the control signals, respectively, whereas the two SOAs are assumed to be two identical devices. In the presence of a control pulse, the switched part of the CW signal appears at the S-port of the output coupler [8]. The S-port output power is given by [8]

$$P_S(t) = \frac{P_{\rm CW}}{4}[G_1(t) + G_{\rm CW} - 2\sqrt{G_1(t)G_{\rm CW}} \cdot \cos(\Delta\varphi(t))]. \tag{1}$$

In (1), $P_{\rm CW}$ is the CW signal input optical power, $G_1(t)$ and $G_{\rm CW}$ are the upper and lower branch SOA gains, respectively, and $\Delta\varphi(t)$ is the phase difference between the two CW components provided by

$$\Delta\varphi(t) = -\frac{\alpha}{2}\ln[G_1(t)/G_{\rm CW}] \tag{2}$$

with α denoting the SOAs linewidth enhancement factor.

The $G_{\rm CW}$ gain is the time-independent equilibrium gain since no control pulse is inserted into the lower branch SOA. Considering the SOA as a spatially concentrated device, the $G_{\rm CW}$

value is determined only be the SOA small-signal gain G_0 and the $P_{\rm CW}$ input power [9]. On the other hand, in the case of single control pulse insertion, $G_1(t)$ is provided by [9]

$$G_1(t) = [1 - (1 - (1/G_{\rm CW}))\exp(-U_{\rm in}(t)/U_{\rm sat})]^{-1} \quad (3)$$

where $U_{\rm in}(t)$ is the accumulated injected control pulse energy and $U_{\rm sat}$ is the SOA saturation energy. After the whole pulse has passed through the SOA, the gain recovers to its initial $G_{\rm CW}$ value with the stimulated carrier lifetime constant [1].

In the case of an amplitude modulated control pulse train, the energy of the kth individual control pulse that affects the SOA at the moment t can be expressed as

$$U_{\rm in}^k(t) = P_0(1 + m \cdot \cos(\Omega \cdot k \cdot T)) \cdot \int_{-\infty}^{t} a(t')dt'. \quad (4)$$

In (4), $a(t)$ represents the pulse waveform, P_0 is the average peak power value across the whole control signal sequence, m is the modulation depth index, Ω is the modulation frequency, and T is the bit period. If T is greater than the stimulated carrier recombination time, $G_1^k(t)$ will recover back to the initial $G_{\rm CW}$ value after each control pulse, allowing for the validity of (3) for the whole bit sequence. This assumption can be valid even up to 40-Gb/s data rates [1].

The amplitude modulation at the output of the gate is obtained by calculating the peak power of every switched pulse. When the whole control pulse energy has been inserted into the SOA, the time-dependent integral contained in (4) can be replaced with a constant value A. The peak power of the kth switched pulse is obtained by replacing the integral with A, using (4) into (3), and then (3) and (2) into (1).

The switched pulse peak power expression is then expanded to a Taylor series around the zero value of m, as a sum of a dc optical power component and an oscillating, modulating power term at Ω. The amplitude modulation depth index at the output of the gate $m_{o/p}$ is defined as the ratio of the modulating power at Ω to the dc optical power. The resulting expression is a function of $m, \alpha, G_{\rm CW}$, of the average minimum gain value $G_1|_{m=0}$ and of the first derivative of $G_1(m)$ at $m = 0$.

For optimized switching performance, the average peak power P_0 has to correspond to an induced phase shift of π. This requirement leads to $G_1|_{m=0} = G_{\rm CW} \cdot \exp(-2\pi/\alpha)$ when applied to (2). The fractional expression of the amplitude modulation depth index $m_{o/p}$ at the output concludes then to

$$m_{\rm o/p} = \frac{\left(1 + \exp\left(\frac{\pi}{\alpha}\right)\right) \cdot \exp\left(-\frac{2\pi}{\alpha}\right) \cdot \left(1 - G_{\rm CW} \cdot \exp\left(-\frac{2\pi}{\alpha}\right)\right)}{1 + \exp\left(-\frac{2\pi}{\alpha}\right) + 2 \cdot \exp\left(-\frac{\pi}{\alpha}\right)} \cdot \ln\left(\frac{1 - \frac{1}{G_{\rm CW}}}{1 - \frac{1}{G_{\rm CW}} \cdot \exp\left(\frac{2\pi}{\alpha}\right)}\right) \cdot m. \quad (5)$$

Equation (5) provides the transfer function characteristics of the gate for every amplitude modulating signal frequency component. It shows that the relation between output and input amplitude modulation is linear, depending only on the gain $G_{\rm CW}$ and the α-parameter of the SOA. Furthermore, the absolute value of this constant is always less than one.

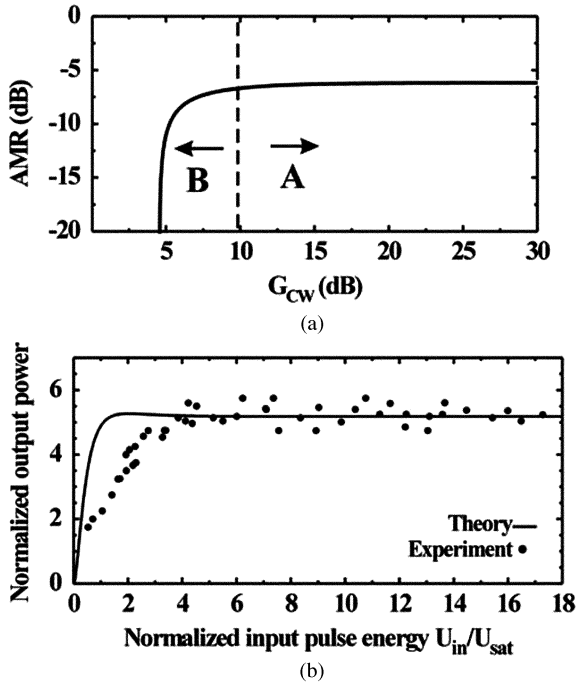

Fig. 2. (a) Theoretically calculated AMR at the output of the MZI gate for various $G_{\rm CW}$ values. (b) Theoretical (solid line, for $G_{\rm CW} = 2.85$) and experimental (black circles) power-limiting output power versus input pulse energy transfer function.

Let us define the amplitude modulation reduction (AMR) index as AMR $= 10 \cdot \log|m_{\rm o/p}/m|$. Fig. 2(a) shows the graphical representation of AMR for different $G_{\rm CW}$ values in log scale. It can be seen that when the SOA operates in the high gain Region A, corresponding to gain values between 10 and 30 dB, a nearly constant AMR of about 6 dB is obtained. However, as the gain decreases below 10 dB and the SOA is forced to operate in the low gain Region B of the graph, the AMR can exceed 10 dB. This reduction becomes more pronounced as the $G_{\rm CW}$ value approaches the limit $10 \cdot \log[\exp(2\pi/\alpha)]$. This limit is dictated by the requirement for π phase shift even when the SOA operates at the transparency point, i.e., $G_1|_{m=0} = 1$.

The output versus input power transfer function of the gate is obtained by inserting (3) and (2) into (1), regarding $G_{\rm CW}$ and $U_{\rm in}$ as the variables. As long as the $G_{\rm CW}$ value is within the operational regime indicated by Region A in Fig. 2(a), the transfer function has the well-known near sinusoidal form that is responsible for the 6-dB AMR. However, when the value of $G_{\rm CW}$ lies within the range indicated by Region B, the switched power curve takes a strongly nonlinear form that is almost parallel to the x axis. The solid line in Fig. 2(b) shows the theoretically obtained transfer function of the gate for a linear $G_{\rm CW}$ value of 2.85, very close to its linear gain limit, which clearly possesses the characteristics of a power-limiting device. The output power is clamped to a constant level irrespective of the inserted control pulse energy after a specific $U_{\rm in}$ threshold. For all the theoretically obtained graphs of Fig. 2, the α-parameter was chosen to have a typical value of six, resulting in a linear gain limit of $\exp(2\pi/6) \approx 2.848$.

Fig. 3 shows the experimental setup of the power-limiter. A distributed feedback laser source (LD1) provides 8-ps pulses at 1.290 75 GHz that are inserted into a Fabry–Pérot filter

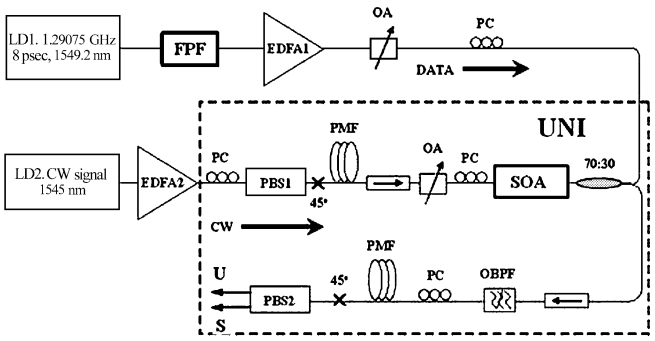

Fig. 3. Experimental setup. OA: optical attenuator. PC: polarization controller. PBS: polarization beam splitter. OBPF: optical bandpass filter. PMF: polarization-maintaining fiber.

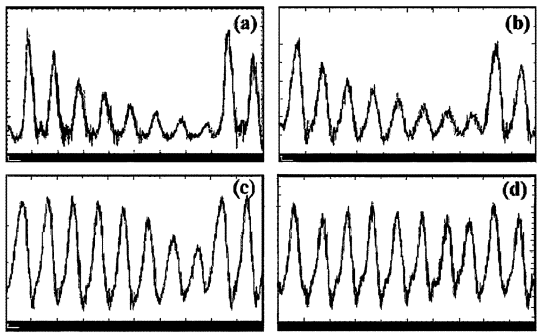

Fig. 4. (a) Control pulse sequence at the FPF output, (b), (c), (d) corresponding switched pulse trains at the output of the gate for a control power of (b) 200, (c) 600, and (d) 800 μW. Time base: 100 ps/div.

(FPF) with a free spectral range of 10.326 GHz. In this way, a 10.326-GHz clock signal with controllable amplitude modulation is provided at the output of the filter and is then launched as the control signal into the UNI gate. The gate is optimized for operation at 10.326 Gb/s [6] and is powered by a CW signal at 1545 nm (LD2), which determines the saturation level of the SOA. The active element is a 1.5-mm bulk SOA with 30-dB peak small signal gain at 1560 nm and 80-ps recovery time, when driven with 700-mA dc current. The $U_{\rm sat}$ parameter of the amplifier was found to be approximately 10 fJ.

Fig. 4(a) shows the control pulse sequence as it appears at the output of the FPF. The amplitude modulation on these pulses has a period of 8 bits, can be easily calculated, as it originates from the memory properties of the filter, and has a maximum value of approximately 9 dB, defined as the highest to the lowest pulse ratio. This provides a controllable way of measuring the energy of every individual pulse for a given average power of the control signal inserted into the SOA. Fig. 4(b), (c), and (d) illustrates the corresponding switched signal for three indicative control signal powers inserted into the SOA, namely 200, 600, and 800 μW, respectively. It is evident that the amplitude modulation imposed on the switched pulses reduces to 7, 2.4, and 0.8 dB, respectively, as the control signal power increases, revealing a maximum AMR of 8.2 dB. The CW power level that was used for deeply saturating the SOA was 1 mW.

Using the same CW power level, this measurement procedure was repeated for different control signal power values inserted into the SOA in order to cover a broad control pulse energy range. The black circles Fig. 2(b) form the experimentally obtained normalized output versus input power transfer function, after correlating the switched output pulse energy to the respective control pulse energy for every injected control signal average power level. Comparison between this curve and the solid line Fig. 2(b) shows good agreement between theory and experiment and confirms the successful demonstration of the power-limiting properties of saturated optical gates, indicating their potential to provide increased input pulse power fluctuation suppression in excess of 10 dB. Minor variations between the two curves, like the $U_{\rm in}/U_{\rm sat}$ threshold for obtaining the "flat" response, are presumably due to the nonnegligible internal losses of the SOA. It is worth mentioning that power-limiting is obtained while the switch still exhibits 2R regenerative properties [7], taking advantage of the typical sinusoidal transfer function shape below the $U_{\rm in}/U_{\rm sat}$ threshold value.

It should be noted that the use of different interferometric structures for the theoretical and experimental analysis, respectively, does not impair the conclusions of this study or the validity of the agreement, since both configurations rely on the same principle of operation due to their interferometric arrangement. For the power-limiting operation, the key parameter is only the degree of saturation of the SOA, rather than the specific architecture of the interferometer.

III. Conclusion

We have presented both theoretically and experimentally the successful operation of a deeply saturated SOA-based interferometric gate as an optical power-limiter. This circuit can lead to novel functional subsystems for optical packet switching applications [6], [7] and can in principle offer enhanced performance characteristics to optical signal processing [10] and optical code-division multiple-access systems [3].

References

[1] R. J. Manning and D. A. O. Davies, "Three-wavelength device for all-optical signal processing," *Opt. Lett.*, vol. 19, pp. 889–891, June 1994.

[2] L. Brzozowski and E. H. Sargent, "All-optical analog-to-digital converters, hardlimiters, and logic gates," *J. Lightwave Technol.*, vol. 19, pp. 114–119, Jan. 2001.

[3] J.-J. Chen and G.-C. Yang, "CDMA fiber-optic systems with optical hard limiters," *J. Lightwave Technol.*, vol. 19, pp. 950–958, July 2001.

[4] J. Leuthold *et al.*, "Nonblocking all-optical cross connect based on regenerative all-optical wavelength converter in a transparent demonstration over 42 nodes and 16 800 km," *J. Lightwave Technol.*, vol. 21, pp. 2863–2870, Nov. 2003.

[5] J.-Y. Emery *et al.*, "Increased input power dynamic range of Mach–Zehnder wavelength converter using a semiconductor optical amplifier power equalizer with 8 dBm output saturation power," *Electron. Lett.*, vol. 35, pp. 995–996, June 1999.

[6] C. Bintjas, K. Vlachos, N. Pleros, and H. Avramopoulos, "Ultrafast nonlinear interferometer (UNI)-based digital optical circuits and their use in packet switching," *J. Lightwave Technol.*, vol. 21, pp. 2629–2637, Nov. 2003.

[7] G. T. Kanellos *et al.*, "Clock and data recovery circuit for 10 Gb/s asynchronous optical packets," *IEEE Photon. Technol. Lett.*, vol. 15, pp. 1666–1668, Nov. 2003.

[8] L. Xu *et al.*, "All-optical data format conversion between RZ and NRZ based on a Mach–Zehnder interferometric wavelength converter," *IEEE Photon. Technol. Lett.*, vol. 15, pp. 308–310, Feb. 2003.

[9] G. P. Agrawal and N. A. Olsson, "Self-phase modulation and spectral broadening of optical pulses in semiconductor laser amplifiers," *IEEE J. Quantum Electron.*, vol. 25, pp. 2297–2306, Nov. 1989.

[10] N. Pleros *et al.*, "Recipe for intensity modulation reduction in SOA-based interferometric switches," *J. Lightwave Technol.*, submitted for publication.